Annals of Diagnostic Pathology 40 (2019) 1–6

Contents lists available at ScienceDirect

Annals of Diagnostic Pathology

journal homepage: www.elsevier.com/locate/anndiagpath

Original Contribution

Amyloid and hyaline globules in undifferentiated nasopharyngeal carcinoma☆

Irfan Sagir Khan[a], Kwok Seng Loh[b], Fredrik Petersson[a,*]

[a] Department of Pathology, National University Health System, Singapore
[b] Department of Otolaryngology - Head and Neck Surgery, National University Health System, Singapore

ARTICLE INFO

Keywords:
Nasopharynx
Carcinoma
Nasopharyngeal carcinoma
Undifferentiated carcinoma
Amyloid
Hyaline globules
Epstein Barr virus

ABSTRACT

We characterize the clinicopathological features of two patients (one 38 year old woman and one 42 year old man, both of Chinese ethnicity) with Epstein Barr Virus positive non-keratinizing nasopharyngeal carcinoma from an endemic region with prominent presence of amyloid and one case with both amyloid and abundant intracytoplasmic hyaline globules. The amyloid material was positive for Congo red and showed apple green birefringence when examined under polarized light. The amyloid was immunoreactive for cytokeratins and was located both intra- and extracellularly. Frequently the amyloid had a light microscopical spherical appearance and displayed peripheral radiating fibrils from a central homogenous core. One of the patients had a unique presentation of nasopharyngeal carcinoma with perceived hemoptysis and coughing up two pieces of tumor tissue. In reality, the nasopharyngeal tumor was polypoid and the two fragments were pinched of from the main tumor mass.

1. Introduction

The majority (> 90%) of non-keratinizing carcinomas of the nasopharynx (NPC) display, in addition to nuclear presence of Epstein Barr virus RNA (EBER), a spectrum of characteristic histomorphological patterns. This includes at one end, tumor cells arranged in syncytial sheets (Regaud-pattern), and at the other end of the spectrum small nests and isolated malignant epithelial cells (Schmincke-pattern), admixed with a variable number of reactive lymphocytes and plasma cells. However, in a significant minority (up to 10% of cases), NPC exhibits a variety of uncommon histopathological patterns, including spindle cells, clear cells, presence of bizarre (Reed-Sternberg-like) tumor cells, non-caseating granulomas, a papillary architecture, significant number of eosinophilic or neutrophilic granulocytes, a desmoplastic stromal reaction frequently with paucity of reactive mononuclear inflammatory cells and a predominance of spindle cells [1]. Very rarely, NPC may display a cord-like, reticular arrangement of tumor cells associated with significant myxoid substances in the stroma or adenomatous differentiation [2,3]. Two distinctly uncommon features in NPC are the presence of amyloid and eosinophilic globules. We herein present two cases of NPC with a significant component of amyloid and one case with both amyloid and prominent intracytoplasmic hyaline globules associated with clear cell change. The tumor with both amyloid and intracytoplasmic hyaline globules presented in a patient who sought medical attention because he perceived he had coughed up blood together with two lumps of tissue.

2. Case 1

A 38 year old non-smoking Chinese woman without any significant past history presented with bilateral neck swelling of one year duration. Clinical examination revealed enlarged cervical lymph nodes. Fine needle aspiration cytology (FNAC) of the lymph nodes was done and the findings are discussed below. Subsequently, the patient underwent a computerized tomography (CT) scan of the nasopharynx and neck, which showed a mass in the roof of the left nasopharynx, obliterating the left fossa of Rosenmuller and torus tubarius. The mass was extending into the left parapharyngeal fat with encasement of the left carotid sheath and erosion of the skull base. Multiple bilateral enlarged lymph nodes were identified. The patient underwent a biopsy of the nasopharyngeal mass. A magnetic resonance imaging (MRI) scan of the nasopharynx confirmed the presence of a mass in the left nasopharynx as well as bilateral enlarged cervical lymph nodes (Fig. 1A, B). A positron emission tomography (PET) scan showed FDG avid lesions

☆ The authors have no conflict of interest. No funding was received.
It is our institution's policy not to require formal ethical approval for reports on up to two patients.

* Corresponding author at: Department of Pathology, National University Health System, 5 Lower Kent Ridge Road, 119074, Singapore.
E-mail address: fredrikpetersson@live.se (F. Petersson).

https://doi.org/10.1016/j.anndiagpath.2019.02.016

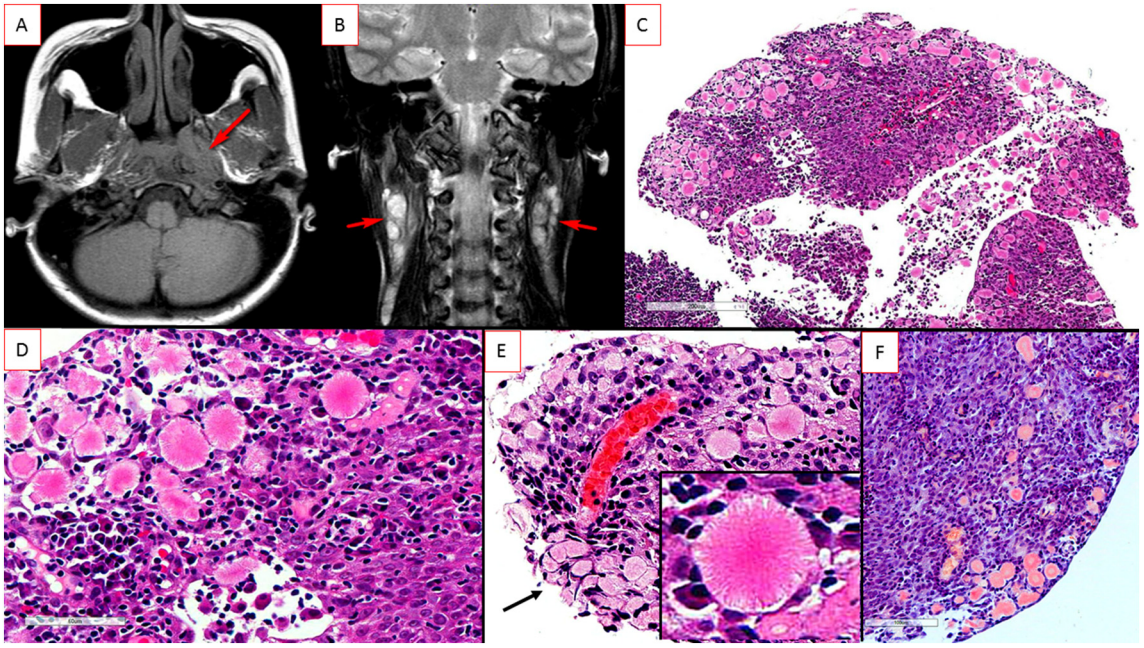

Fig. 1. MRI-scan of patient 1 showed a left sided nasopharyngeal mass and bilateral cervical lymphadenopathy (A and B; arrows). Hematoxylin and Eosin stained sections from the biopsy of the nasopharyngeal mass (Case 1) contained tumor with numerous intra- and extracellular round eosinophilic structures (C and D). In several areas the intracellular eosinophilic material was so abundant that the nuclei were pushed to the periphery (E; arrow). Frequently the round eosinophilic material displayed radiating fibrils from a central homogenous core (E; inset). The round eosinophilic structures were positive for Congo red (F).

corresponding to the nasopharyngeal mass and bilateral enlarged cervical lymph nodes. There was no evidence of distant metastatic disease. The patient underwent chemoradiotherapy. There has been no evidence of recurrence or disease progression at 6 years follow-up.

2.1. Microscopic findings

FNA of the cervical lymph node showed cellular smears with numerous clusters and crowded sheets of atypical cells in a background of mixed population of lymphocytes and plasma cells. The atypical cells displayed enlarged, irregular nuclei and moderate amount of cytoplasm. No necrosis was identified. There were few aggregates of isolated rounded glass like semi-transparent crystalloid-like structure noted.

The biopsy material was composed of two fragments of tissue measuring 0.3 and 0.4 cm. Histological sections showed a highly cellular tumor composed of syncytial sheets of malignant epithelial cells with round enlarged nuclei, prominent nucleoli and moderate amounts of cytoplasm. The stroma contained a lymphoplasmacytic inflammatory infiltrate which also were admixed with the tumor cells. There were several foci that contained numerous both extra- and intracellular spherical weakly eosinophilic round structures (Fig. 1C, D). This weakly eosinophilic material, was occasionally so abundant that the nuclei were displaced to the periphery, forming a crescent giving rise to a signet ring cell-like appearance (Fig. 1E).

The majority of these eosinophilic spherical structures were composed of thin, straight fibrillary structures radiating from a central core which had a more homogenous appearance than the periphery (Fig. 1E).

2.2. Immunohistochemistry, in-situ hybridization and histochemistry

In the immunohistochemical study, tumor cells strongly expressed cytokeratins (AE1–3). The intracytoplasmic material was positive for Congo red and this material showed distinct apple green birefringence when examined under polarized light (Figs. 1F, 2A). Also the spherical weakly eosinophilic structures displayed immunoreactivity for cytokeratins (Fig. 2B). Chromogenic in-situ hybridization for EBV (EBER-ISH) revealed strong nuclear positivity in all neoplastic cells and also highlighted the “signet ring cell-like appearance” of those neoplastic cells which had their cytoplasm distended by the eosinophilic material (Fig. 2C). Masson's trichrome (MT) showed variable dark blue staining in the homogenous center of the weakly esonophilic material, but the peripheral radiating fibrils did not take up any color. Alcian blue (AB) showed faint bluish staining of the radiating fibrils, but not the homogenous center. These structures were also negative for Gomori Methenamine-Silver (GMS) and Verhoeff-Van Gieson stains.

3. Case 2

A 42 year old non-smoking Chinese man without any significant past medical history, presented to the emergency department after an episode of what he perceived to be hemoptysis with expectoration of two tissue fragment measuring 2 and 1 cm, respectively. This episode had been preceded by nasal congestion of one week duration and a single episode of epistaxis. Nasal examination showed traces of blood clots with no active bleeding. He was referred to the respiratory medicine clinic. The two tissue fragments were sent for histopathological assessment. A bronchoscopic and CT-scan of the thorax were unremarkable. A CT scan of the head and neck showed a mass in the right nasopharynx, crossing the midline and involving the right fossa of Rosenmuller with extension into the posterior aspect of the right nasal cavity anteriorly (Fig. 3A). The patient was immediately referred to the department of otorhinolaryngology and underwent a clinical examination which revealed a mass arising from the right nasopharynx and extending into the posterior aspect of the right nasal cavity. This tumor was biopsied. A subsequent MRI scan of the nasopharynx and neck confirmed the CT findings. A staging PET scan showed confirmed a hypermetabolic right nasopharyngeal lesion and showed mildly FDG avid bilateral cervical lymph nodes. There was no evidence of distant metastatic disease. The patient underwent chemoradiotherapy and there has been no evidence of recurrence or disease progression at 22 months follow-up.

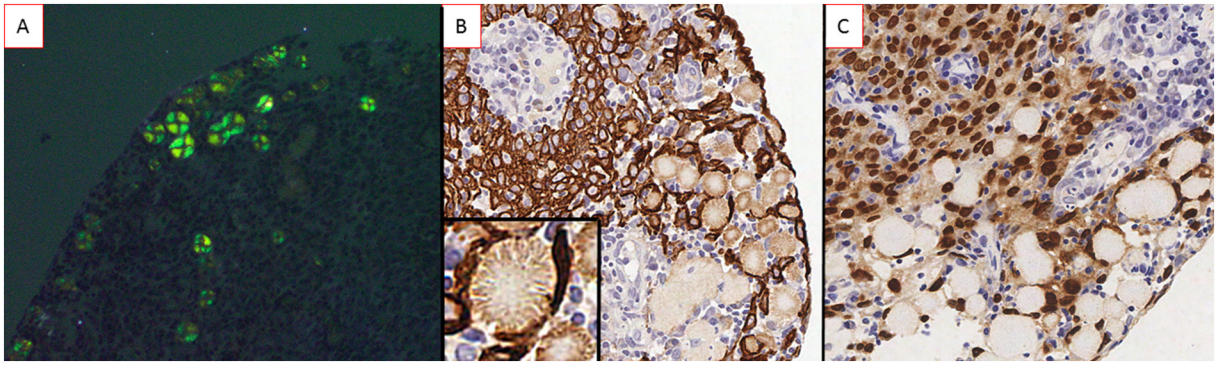

Fig. 2. The Congo red positive round material in the nasopharyngeal biopsy in patient 1 showed apple green birefringence when examined under polarized light (A), and was immunohistochemically positive for cytokeratins (B); high power magnification of the cytokeratin positive round material highlighting the peripheral radiating fibrillary structure (B; inset). The tumor cells showed strong positivity for EBV (EBER) on chromogenic in-situ hybridization (C). Please note the signet ring cell-like appearance in tumor cells with the cytoplasm distended by the amyloid material.

3.1. Microscopic findings

The perceived expectorated material (with some blood) was sent for histopathological assessment. The material was composed of two fragments of whitish fibrous tissue, the larger fragment measuring 2.0 × 1.6 × 1.2 cm and the smaller fragment measuring 1.0 × 0.4 × 0.1 cm. Sections showed well preserved tissue; featuring a polypoid tumor (Fig. 3B). The tumor was composed of broad anastomosing trabeculae and sheets of tumor cells set in a stroma with a dense lymphoplasmacytic infiltrate. The tumor cells displayed predominantly moderate nuclear pleomorphism, and vaguely eosinophilic cytoplasm. Some tumor cells exhibited pronounced nuclear enlargement and pleomorphism. In several areas, the tumor cells displayed prominent presence of intracytoplasmic strongly eosinophilic non-refractile hyaline globules (Fig. 3C, D). Dispersed within the tumor were multiple areas with neoplastic cells containing both intra- and extracellular partly refractile eosinophilic material (Fig. 3E). When this material was intracellular it had a spherical appearance. Some of these intracellular round eosinophilic structures displayed radiating thin fibrillary structures from a homogenous core. This weakly eosinophilic material was also seen extracellularly, and was then frequently larger in size, irregular in shape and generally homogenously amorphous with no radiating fibrillary structures. In several areas neoplastic cells with eosinophilic hyaline globules merged with neoplastic cells containing the weaker eosinophilic material.

The biopsy from the right nasopharyngeal tumor was composed of one fragment of tissue measuring 0.7 cm in maximum dimension (Fig. 4A). The biopsy contained malignant tumor with the same histopathologic features as in the specimen described above, i.e. composed of sheets of tumor cells with moderate to severe nuclear pleomorphism, prominent nucleoli and weakly eosinophilic cytoplasm admixed with lymphocytes and plasma cells. Also in this biopsy, were there several aggregates of neoplastic cells of which some exhibited clear cell change containing weakly eosinophilic material, (Fig. 4B). The round weakly eosinophilic displayed material which frequently showed a fibrillar structure radiating from a central homogenous core. Only very few

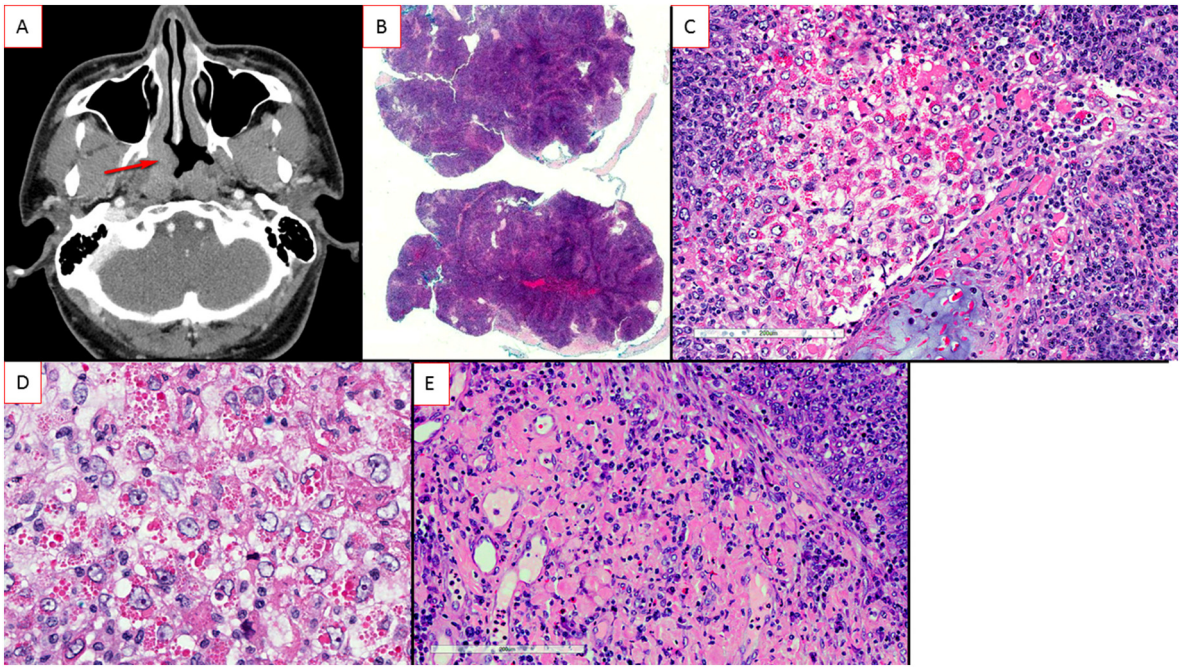

Fig. 3. CT-scan of patient 2 showed a right sided nasopharyngeal mass reaching the posterior aspect of the nasal cavity (A, arrow). Low power magnification (Hematoxylin and Eosin) of the pieces of tumor tissue that the patient perceived to have coughed up together with some blood (B). Hematoxylin and Eosin stained sections from the tumor tissue that the patient perceived to have coughed up contained multiple areas where the neoplastic cells contained abundant intracellular hyaline globules (C and D). The tumor tissue also contained multiple foci with intra- and extracellular eosinophilic material (E).

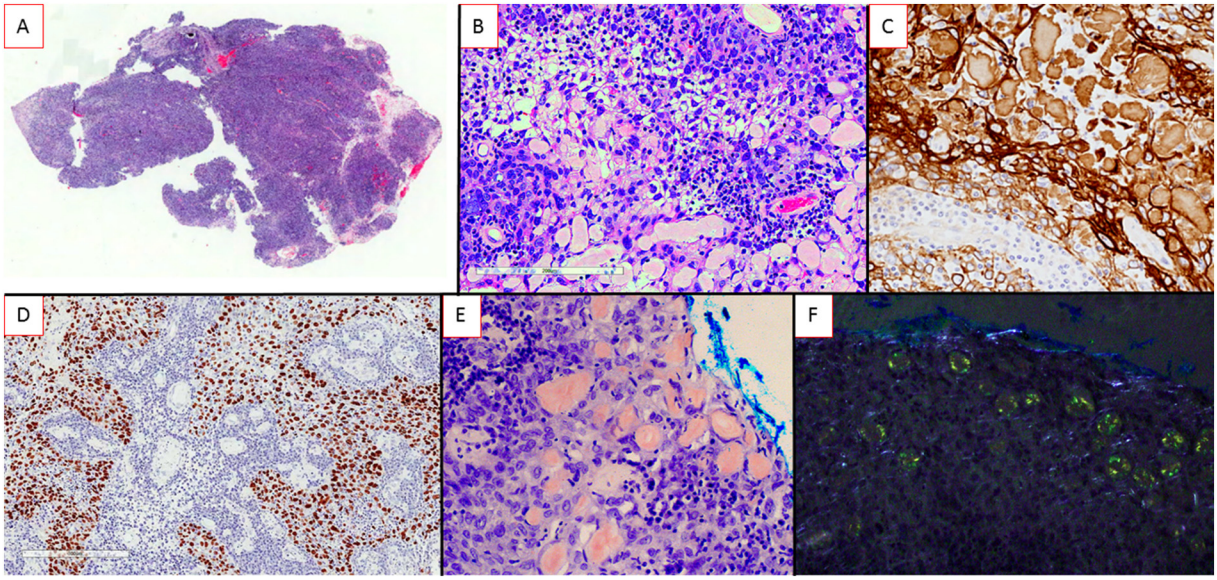

Fig. 4. Low power view of a Hematoxylin and Eosin stained section from the biopsy from the right sided nasopharyngeal mass of patient 2 (A). The biopsy contained areas where the tumor cells displayed clear cell change and intracellular weakly eosinophilic material (B). The intra- and extracellular material *in the perceived coughed up tumor tissue* (patient 2) was immunoreactive for cytokeratins (C). The tumor cells in the *perceived coughed up tumor tissue* were strongly positive for EBV (D; EBER chromogenic in situ hybridization), and the eosinophilic material was positive for Congo red (E) and showed apple green birefringence when examined under polarized light (F).

intracytoplasmic strongly eosinophilic hyaline globules were detected.

3.2. Immunohistochemistry, in-situ hybridization and histochemistry

The immunohistochemical study of the perceived expectorated/hemoptysed specimen showed that the neoplastic cells diffusely expressed low-molecular weight cytokeratins (AE1–3) and p40. The weakly eosinophilic material (which were present both intra- and extracellularly) displayed immunoreactivity for cytokeratins (AE1–3) (Fig. 4C). The tumor cells showed strong and diffuse nuclear positivity on ISH for EBV (EBER) (Fig. 4D). The eosinophilic spherules were positive for Congo-red (Fig. 4E). The Congo red positive material showed apple green bi-refringence when examined under polarized light (Fig. 4F).

The tumor cells in the nasopharyngeal biopsy showed diffuse strong expression of cytokeratins (AE1–3) and were strongly positive for EBV on chromogenic ISH for EBER (Fig. 5A). EBV-positive nuclear remnants/fragments were seen in areas which extracellular amyloid. Both the intra and extracellular weakly eosinophilic material were positive for Congo-red (with apple green birefringence when examined under polarized light) and displayed immunoreactivity for cytokeratins (AE1–3) (Fig. 5B, C).

4. Discussion

We herein report two cases of undifferentiated nasopharyngeal carcinoma with uncommon histopathological features, namely presence of amyloid and also in one case with a significant component of tumor cells with prominent eosinophilic cytoplasmic globules. In addition, one of the patients (Case 2) presented with a history of perceived hemoptysis and “coughed up” pieces of tumor. Given the clinico-pathologic features of this case, the explanation for this is that the nasopharyngeal tumor was polypoid in nature and was incidentally pinched off the main tumor mass. Anecdotally, patients may cough up fragments of polypoid bronchial tumors, but this presentation of NPC has not, to the best of our knowledge, been reported previously, and has not been experienced at our center, which is a tertiary cancer center in a country where NPC is endemic. Of interest, the rare lymphoepithelial carcinoma (analogous to non-keratinizing nasopharyngeal carcinoma) of the lung may be positive for EBV and has rarely been described to contain amyloid [4,5].

WHO classifies nasopharyngeal carcinoma (NPC) into keratinizing (squamous cell), non-keratinizing (including differentiated and undifferentiated variants) and basaloid (squamous) types of carcinoma. This is not a pure “histological” classification system, but in addition to morphology, it also embraces epidemiological, virological and prognostic aspects [6]. Keratinizing NPC (K-NPC) shows histological features that are no different from conventional SCC at any other site, i.e. with malignant cells displaying evidence of keratinocytic differentiation in the form of intercellular junctions and variable keratin formation. The rare basaloid (squamous cell) carcinoma is a variant of NPC that is histopathologically analogous to basaloid SCC at other sites, which was first described by Wain et al. [7]. This tumor is enigmatic in that its biology and prognosis appear to be site dependent. In the nasopharynx this neoplasm is associated with EBV [8], but in the oropharynx it is commonly associated with transcriptionally active HPV and in other Head and Neck sites there is no strong to any relevant oncogenic virus [9].

The remarkably higher incidence of NPC among the Chinese, especially in south China and South Eastern Asia is mainly attributed to the non-keratinizing type which has an almost 100% association with EBV and is characterized by marked sensitivity to radiotherapy [1]. NK-NPC characteristically harbors a significant lymphoplasmacytic infiltrate. When this is especially prominent and the neoplastic epithelial cells display a small nested or individual cell (Regaud) pattern, diagnostic difficulties may ensue and immunohistochemistry is frequently needed to highlight the epithelial component. On the contrary, when NK-NPC shows the sheet-like (Schmincke) pattern composed of large undifferentiated neoplastic cells, the possibility of a large cell lymphoma needs to be ruled out. However, NK-NPC may exhibit light-microscopical features that deviate from the standard text book appearance. Uncommonly encountered morphological variants of NK-NPC include tumors with a predominance of spindle cells, clear cells, pleomorphic cells, desmoplastic stroma, with granulomas, marked stromal infiltration of eosinophilic or neutrophilic granulocytes and prominent papillarity [1]. Very rarely, a reticular myxoid pattern or adenomatous

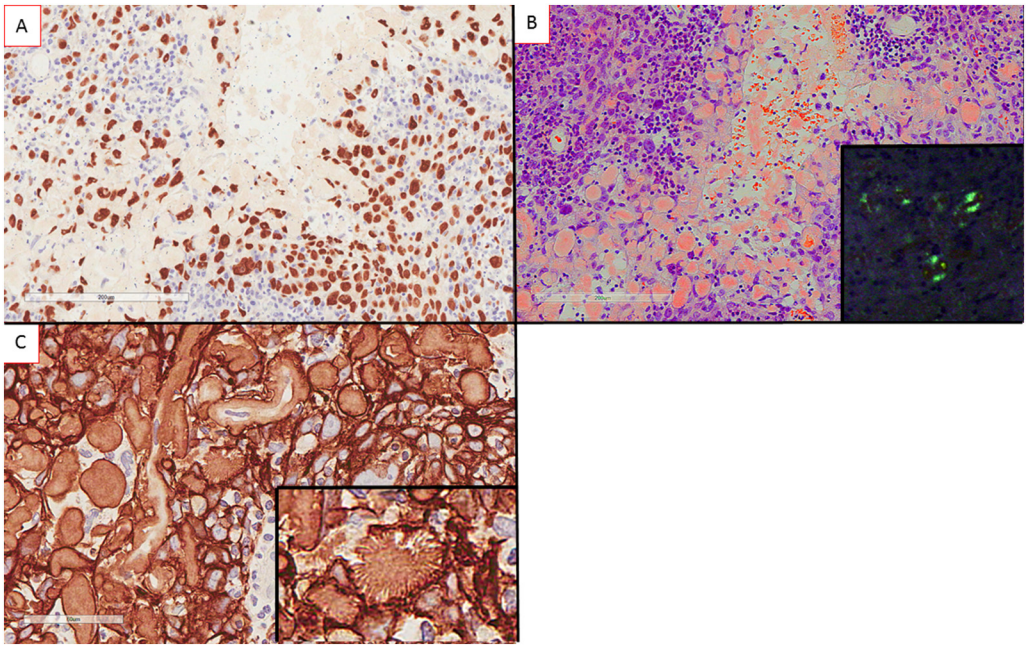

Fig. 5. The tumor cells in the biopsy from the right sided nasopharyngeal mass (patient 2) were strongly positive for EBV (A; EBER chromogenic in situ hybridization) and the eosinophilic material was positive for Congo red (B), with apple green birefringence when examined under polarized light (B; inset) and immunoreactive for cytokeratins (C) which on high-power magnification highlighted the peripheral radiating fibrillary structure (C; inset).

differentiation may be encountered [2,3]. NPC with amyloid and presence of eosinophilic cytoplasmic globules, associated with NPC have previously been described in studies from regions where NPC is endemic [10,11]. Presence of amyloid in NPC has also been mentioned in a few previous review papers on NPC [1,12], as well as in the chapters on NPC in the latest WHO classifications of Head and Neck tumors. Presence of eosinophilic cytoplasmic globules in NPC has, to the best of our knowledge, only been described in one previous study [13].

Tumor-associated amyloid is commonly encountered in medullary carcinoma of the thyroid (where the basic protein constituent is calcitonin possibly admixed with secretogranin-1 and calcitonin gene-related peptide) [14,15], calcifying epithelial odontogenic (Pindborg) tumor, plasma cell neoplasms and lymphomas with plasmacytic differentiation, e.g. some marginal zone lymphomas and lymphoplasmacytic lymphoma. In addition, more or less uncommonly, amyloid has been described in a wide range of neoplasms, for example cutaneous basal cell carcinoma [16], pancreatic endocrine tumors [17], renal angiomyolipoma [18], salivary gland low-grade adenocarcinoma [19] and acinic cell carcinoma [20], endometrial endometrioid adenocarcinoma [21], mammary ductal carcinoma [22], ovarian strumal carcinoid [23], carcinoids (both conventional and atypical) [24,25], pulmonary adenosquamous carcinoma [26] and squamous cell carcinoma of the oral cavity, pharynx, larynx, vagina and uterine cervix [27-31]. The exact details of the biological and chemical details of such amyloidogenic processes in neoplasms are largely unknown. In the case of amyloid formation in medullary thyroid carcinoma (where the bulk of the amyloid contains calcitonin with a fibrillar structure), it has been suggested that a hexapeptide of calcitonin may serve as a possible 'aggregation-prone' peptide, which may play a role in amyloid-formation via self-assembly into amyloid fibrils [32]. The mechanism behind amyloid formation in squamous cell and basal cell carcinomas is different. Several studies have shown that the amyloid in this context is immunohistochemically positive for cytokeratins [16,27,28,31]. The pathogenesis of the amyloid in this context thus strongly suggests that of a change in the three dimensional structure of the cytokeratin intermediate filaments which results in giving the keratin the physical properties of amyloid. However, the exact mechanism behind this is not known. Similarly, primary cutaneous amyloidosis (lichen amyloidosis and macular amyloidosis) is related to transformation of cytokeratin filaments of degenerated/apoptotic epidermal keratinocytes that have been discharged into the superficial dermis [33].

The nodular both intra- and extracellular amyloid deposits seen in our case show distinct similarities to the amyloid in basal cell- and squamous cell carcinoma [16,27,31]. The electron microscopic characterization of the amyloid structures in squamous cell carcinoma by Gondo et al. ("nodular and star-like amyloid deposits") fits well with the features seen in the amyloid in our cases. The idea that the keratin filaments derived from degenerating or dead cells is supported by the morphological findings in our Case 2, where we (A) encountered degenerated tumor cells, occasionally with clear cell change (especially in the biopsy specimen in Case 2) in direct continuity to areas containing where tumor cells had the whole cytoplasm filled with amyloid which blended in with areas of extracellular amyloid and (B) EBV-positive nuclear remnants/fragments in areas which extracellular amyloid. The viability of such a cellular alteration, i.e. tumor cells "overloaded" with intracytoplasmic amyloid is questionable. This is in line with what has been proposed by Hashimoto and Kumakiri as the "the filamentous degeneration theory" in primary cutaneous amyloidosis [34], where sequential electron microscopic observations strongly support the idea that degenerating epidermal cells are discharged into the dermis and cytokeratins are converted into amyloid.

One curious finding on a light microscopical level was the morphological similarity between many of the amyloid structures in our cases to collagenous crystalloids (CC). CC are formed by basement membrane constituents, not only in neoplasm rich in myoepithelial cells, e.g. salivary gland tumors, but also in basaloid squamous cell carcinomas, which also frequently produce basal membrane material [35]. CC are composed of spherical structures with radially arranged needle-shaped fibers. However, the histochemical differences of the fibrillary nodular amyloid structures in NPC and true collagenous crystalloids are striking. CCs are bright blue on staining with Masson-Trichrome and bright red with Verhoeff-Van Gieson stains, respectively. We stained the biopsy in our Case 1 and neither of these histochemical features was evident in the CC-like amyloid globules with radiating fibrils.

The finding of areas with prominent presence of intracytoplasmic hyaline globules in Case 2 is distinctly uncommon in NPC. We are only aware of one previously published case with NPC displaying very limited and focal presence of hyaline cytoplasmic globules [13]. The patient was a 73 year old woman from Taiwan (where NPC is endemic) with a non-keratinizing NPC. As with formation of amyloid, hyaline globules (HG) are regularly seen in some tumors. HG are consistently

identified in yolk sac tumor and Kaposi sarcoma, but has more or less rarely been described in a very wide range of neoplasms [36].

Numerous theories have tried to explain the presence of HG in tumors. Some of the histologic features of the HG; distinct eosinophilia and round shape are similar to the cytoplasmic globules in hepatocytes in patients with alpha1-anti trypsin deficiency which are derived from dilated parts of the endoplasmic reticulum with pathological protein content. Papadimitriou et al. have suggested a “unifying theory” behind the formation of HG [36]. The very similar light microscopical appearance of HG in a wide range of different neoplasms is an observation that begs a simplistic explanation and the authors suggested that the formation of HG may be related to a type of cellular reaction to injury and subsequent cell death. This theory suggests that the formation of HGs is related to apoptosis and have launched the telling concept of the “thanatosome”. This line of thinking ties in nicely with the substantiated theory of amyloid transformation of apoptotic neoplastic cells as seen in our Case 2. We noted cells with eosinophilic globules in close association to and in some areas intermingled with both extracellular amyloid deposits and tumor cells with intracytoplasmic amyloid. As stated above, such areas also contained EBV positive nuclear fragments/remnants.

On a final note, it is important to be aware of that localized nasopharyngeal amyloidosis (not associated with any neoplasm), although being very uncommon, has been well characterized and also recently reviewed by Sakagiannis et al. [37]. In addition, non-systemic, non-neoplastic nasopharyngeal amyloidosis may form a tumor mass and may be associated with cervical deposits of amyloid, thus mimicking NPC with cervical nodal metastatic disease [38]. We have previously encountered a somewhat similar case of tumefactive pharyngeal amyloidosis in a 13 year old girl associated with a sparse plasmacytic component that, however, turned out to be a paucicellular extramedullary plasmacytoma [39].

In conclusion, we have described two cases of EBV positive non-keratinizing nasopharyngeal carcinomas from an endemic region with prominent presence of amyloid and one case with both amyloid and intracytoplasmic hyaline globules. Both of these features are uncommon in NK-NPC and awareness that these morphological changes can occur in nasopharyngeal carcinoma should facilitate establishing the correct diagnosis, especially when faced with limited biopsy material in clinical practice. In both our cases the amyloid material was positive for cytokeratins on immunohistochemistry which is in line with the previously validated idea of amyloidogenic transformation of keratins in degenerating/apoptotic tumor cells, which thus also seems to be the mechanism in formation of amyloid in non-keratinizing nasopharyngeal carcinoma. Finally, for the first time, we document a patient with a unique “pseudohemoptytic” presentation of nasopharyngeal carcinoma.

References

[1] Petersson F. Nasopharyngeal carcinoma: a review. Semin Diagn Pathol 2015;32(1):54–73. https://doi.org/10.1053/j.semdp.2015.02.021.

[2] Petersson F, Vijayadwaja D, Loh KS, Tan KB. Reticular and myxoid non-keratinizing nasopharyngeal carcinoma: an unusual case mimicking a salivary gland carcinoma. Head Neck Pathol 2014;8(3):364–8. https://doi.org/10.1007/s12105-013-0512-6.

[3] Petersson F. Non-keratinizing nasopharyngeal carcinoma with adenomatous differentiation. Head Neck Pathol 2018. https://doi.org/10.1007/s12105-018-0991-6. [Epub ahead of print] PMID: 30523510.

[4] Chan JK, Hui PK, Tsang WY, Law CK, Ma CC, Yip TT, et al. Primary lymphoepithelioma-like carcinoma of the lung. A clinicopathologic study of 11 cases. Cancer 1995;76(3):413–22.

[5] Chan JK, Hui PK, Yip TT, Tsang WY, Law CK, Poon YF, et al. Detection of Epstein-Barr virus only in lymphoepithelial carcinomas among primary carcinomas of the lung. Histopathology 1995;26(6):576–8.

[6] F P alE. WHO Classification of Head and Neck Tumours WHO Classification of Tumours. Lyon: IARC Press. 2017.

[7] Wain SL, Kier R, Vollmer RT, Bossen EH. Basaloid-squamous carcinoma of the tongue, hypopharynx, and larynx: report of 10 cases. Hum Pathol 1986;17(11):1158–66.

[8] Wan SK, Chan JK, Lau WH, Yip TT. Basaloid-squamous carcinoma of the nasopharynx. An Epstein-Barr virus-associated neoplasm compared with morphologically identical tumors occurring in other sites. Cancer 1995;76(10):1689–93.

[9] Chernock RD, Lewis Jr. JS, Zhang Q, El-Mofty SK. Human papillomavirus-positive basaloid squamous cell carcinomas of the upper aerodigestive tract: a distinct clinicopathologic and molecular subtype of basaloid squamous cell carcinoma. Hum Pathol 2010;41(7):1016–23. https://doi.org/10.1016/j.humpath.2009.11.015.

[10] Looi LM. Intratumour amyloidosis in Malaysians: an immunohistochemical study. Ann Acad Med Singap 1986;15(1):52–6.

[11] Prathap K, Looi LM, Prasad U. Localized amyloidosis in nasopharyngeal carcinoma. Histopathology 1984;8(1):27–34.

[12] Thompson LD. Update on nasopharyngeal carcinoma. Head Neck Pathol 2007;1(1):81–6. https://doi.org/10.1007/s12105-007-0012-7.

[13] Lee LY, Kuo TT. Hyaline globules in a nasopharyngeal carcinoma. Int J Surg Pathol 2013;21(1):44. https://doi.org/10.1177/1066896912458831.

[14] Erickson LA, Vrana JA, Theis J, Rivera M, Lloyd RV, McPhail E, et al. Analysis of amyloid in medullary thyroid carcinoma by mass spectrometry-based proteomic analysis. Endocr Pathol 2015;26(4):291–5. https://doi.org/10.1007/s12022-015-9390-7.

[15] Khurana R, Agarwal A, Bajpai VK, Verma N, Sharma AK, Gupta RP, et al. Unraveling the amyloid associated with human medullary thyroid carcinoma. Endocrinology 2004;145(12):5465–70. https://doi.org/10.1210/en.2004-0780.

[16] Satti MB, Azzopardi JG. Amyloid deposits in basal cell carcinoma of the skin. A pathologic study of 199 cases. J Am Acad Dermatol 1990;22(6 Pt 1):1082–7.

[17] Shintaku M, Tado H, Inayama K, Murakami T, Suzuki T. Ductulo-insular pancreatic endocrine tumor with amyloid deposition: report of a case. Pathol Int 2015;65(4):197–201. https://doi.org/10.1111/pin.12255.

[18] Toyoda M, Kudo M, Ebihara Y. Amyloid deposition in renal angiomyolipoma. Pathol Int 1999;49(2):180–4.

[19] Yang GC, Kuhel WI, Scognamiglio T. Amyloid-rich low grade adenocarcinoma of the parotid: fine-needle aspiration cytology with histologic correlations. Diagn Cytopathol 2014;42(9):798–801. https://doi.org/10.1002/dc.23099.

[20] Drut R, Gimenez PO. Acinic cell carcinoma of salivary gland with massive deposits of globular amyloid. Int J Surg Pathol 2008;16(2):202–7. https://doi.org/10.1177/1066896907306771.

[21] Kotru M, Chandra H, Singh N, Bhatia A. Localized amyloidosis in endometrioid carcinoma of the uterus: a rare association. Arch Gynecol Obstet 2007;276(4):383–4. https://doi.org/10.1007/s00404-007-0357-x.

[22] Santini D, Pasquinelli G, Alberghini M, Martinelli GN, Taffurelli M. Invasive breast carcinoma with granulomatous response and deposition of unusual amyloid. J Clin Pathol 1992;45(10):885–8.

[23] Morgan K, Wells M, Scott JS. Ovarian strumal carcinoid tumor with amyloid stroma—report of a case with 20-year follow-up. Gynecol Oncol 1985;22(1):121–8.

[24] Al-brahim NY, Radhi JM, Marcaccio MJ. Ampullary carcinoid with amyloid stroma. Histopathology 2005;47(5):537–8. https://doi.org/10.1111/j.1365-2559.2005.02145.x.

[25] Abe Y, Utsunomiya H, Tsutsumi Y. Atypical carcinoid tumor of the lung with amyloid stroma. Acta Pathol Jpn 1992;42(4):286–92.

[26] Yousem SA. Pulmonary adenosquamous carcinomas with amyloid-like stroma. Mod Pathol 1989;2(5):420–6.

[27] Ueno T, Hoshii Y, Cui D, Kawano H, Gondo T, Takahashi M, et al. Immunohistochemical study of cytokeratins in amyloid deposits associated with squamous cell carcinoma and dysplasia in the oral cavity, pharynx and larynx. Pathol Int 2003;53(5):265–9.

[28] Gondo T, Ishihara T, Kawano H, Uchino F, Takahashi M, Iwata T, et al. Localized amyloidosis in squamous cell carcinoma of uterine cervix: electron microscopic features of nodular and star-like amyloid deposits. Virchows Arch A Pathol Anat Histopathol 1993;422(3):225–31.

[29] Tsang WY, Chan JK. Amyloid-producing squamous cell carcinoma of the uterine cervix. Arch Pathol Lab Med 1993;117(2):199–201.

[30] Aho HJ, Talve L, Maenpaa J. Acantholytic squamous cell carcinoma of the uterine cervix with amyloid deposition. Int J Gynecol Pathol 1992;11(2):150–5.

[31] Hsueh S, Kuo TT. Amyloid in squamous cell carcinoma of the vagina: immunohistochemical study with monoclonal anti-keratin antibodies. Int J Gynecol Pathol 1986;5(4):357–61.

[32] Iconomidou VA, Leontis A, Hoenger A, Hamodrakas SJ. Identification of a novel ‘aggregation-prone’/‘amyloidogenic determinant’ peptide in the sequence of the highly amyloidogenic human calcitonin. FEBS Lett 2013;587(6):569–74. https://doi.org/10.1016/j.febslet.2013.01.031.

[33] Chang YT, Liu HN, Wang WJ, Lee DD, Tsai SF. A study of cytokeratin profiles in localized cutaneous amyloids. Arch Dermatol Res 2004;296(2):83–8. https://doi.org/10.1007/s00403-004-0474-3.

[34] Kumakiri M, Hashimoto K. Histogenesis of primary localized cutaneous amyloidosis: sequential change of epidermal keratinocytes to amyloid via filamentous degeneration. J Invest Dermatol 1979;73(2):150–62.

[35] Zamecnik M, Skalova A, Pelikan K, Leivo I. Basaloid squamous carcinoma with collagenous spherules and crystalloids. Ann Diagn Pathol 2001;5(4):233–9. https://doi.org/10.1053/adpa.2001.26979.

[36] Papadimitriou JC, Drachenberg CB, Brenner DS, Newkirk C, Trump BF, Silverberg SG. “Thanatosomes”: a unifying morphogenetic concept for tumor hyaline globules related to apoptosis. Hum Pathol 2000;31(12):1455–65. https://doi.org/10.1053/hupa.2000.20376.

[37] Sakagiannis G, Giotakis E, Thompson LDR. Localized nasopharyngeal amyloidosis: a clinicopathologic series of 7 cases with a literature review. Head Neck Pathol 2018;12(4):542–7. https://doi.org/10.1007/s12105-017-0880-4.

[38] Zhuang YL, Tsai TL, Lin CZ. Localized amyloid deposition in the nasopharynx and neck, mimicking nasopharyngeal carcinoma with neck metastasis. J Chin Med Assoc 2005;68(3):142–5. https://doi.org/10.1016/S1726-4901(09)70236-9.

[39] Tan CL, Tan SH, Ng SB, Petersson F. Expect the unexpected: report of a case of pediatric pharyngeal extraosseous plasmacytoma with tumefactive amyloidosis (“amyloidoma”) and a review of the literature. Head Neck Pathol 2015;9(4):431–5. https://doi.org/10.1007/s12105-015-0614-4.